FUDMA Journal of Sciences (FJS)
ISSN online: 2616-1370
ISSN print: 2645 - 2944
Vol. 7 No. 2, April, 2023, pp 9 - 18
DOI: https://doi.org/10.33003/fjs-2023-0702-1398

CONVECTIVE HEAT AND CASSON NANOFLUID FLOW OVER A VERTICAL PLATE WITH HEAT SOURCE

[1]Sheid A. Momohjimoh, *[1,2]Oyem O. Anselm, [1]Momoh O. Sheidu, [1]Onojovwo T. Felix

[1] Department of Mathematics, Federal University Lokoja, PMB 1154, Nigeria
[2]Department of Mathematics, Busitema University, P.O. Box 226, Uganda

*Corresponding authors' email: anselmoyemfulokoja@gmail.com

ABSTRACT

This paper considers the Casson nanofluid flow of a free convective heat transfer with heat source over a vertical plate and its thermophysical properties. The governing partial differential equations were reduced to couple nonlinear ordinary differential equations using similarity variables. The couple nonlinear ordinary differential equations were solved numerically using Runge-Kutta fourth order method with shooting technique and implemented using MatLab. The effects of various non-dimensional governing parameter namely, Prandtl number, Biot number, Grashof number, heat source parameter, skin-friction coefficient, Nusselt number and Sherwood number is analysed for Casson nanofluid flow, discussed and presented graphically. The result showed that heat source parameter increases in skin-friction coefficient, velocity and temperature profiles but, decreases in concentration profiles and Nusselt number.

Keywords: Fluid flow, Nanoparticles, Sherwood number, Skin-friction coefficient, Thermophysical parameters, Vertical Plate

INTRODUCTION

Non-Newtonian fluid which is also a Casson fluid is a shear thinning liquid assumed to have an infinite viscosity at zero rate of shear and a zero viscosity at an infinite rate of shear. Basically, the non-Newtonian behaviour has much industrial and scientific importance (Blair, 1959). Some of these applicable areas are in automobile, steam electric power generation, energy system, and electronic device cooling, nuclear reactor, thermal devices, medicine and rapid methane hydrate, characterization and diagnosis of diseases. Nanoparticles, which are non-Newtonian, have gained global recognition in the area of research by scientist in recent times with applications in chemical processes, engineering, thermal sciences and technological processes. Some of these areas of application include thermal system, metal cutting, power pump, heat-flux devices, and in medical sciences like cancer treatment, artificial lungs, heart diseases, among others (Sivashanmugam 2012; ShanthaSheela et al. 2021).

Choi and Eastman (1995) studied thermal conductivity of fluids with nanoparticles. Pramanik (2014) investigated Casson fluid flow and heat transfer past an exponentially porous stretching surface in presence of thermal radiation. Arthur et al. (2015) looked into Casson fluid flow over a vertical porous surface with chemical reaction in the presence of magnetic field. Hussain et al. (2015) studied mhd boundary layer flow of Casson fluid in the presence of nanoparticles. They observed that temperature and nanoparticle concentration fields decreases when the value of Casson parameter enhances. Ullah et al. (2016) analyzed mhd natural convection flow of Casson nanofluid over nonlinearly stretching sheet through porous medium with chemical reaction and thermal radiation. Heat and mass transfer characteristics of mhd Casson fluid flow over a vertical plate in the presence of thermal radiation, chemical reaction and heat source/sink with buoyancy effects was discussed by Vijayaragavan and Kavitha (2017).

Nanofluids have been found useful by several researchers due to its industrial significance such as examine the impact of thermal radiation, heat generation and chemical reaction of a nanofluid, organic fluids, bio-fluids, pharmaceutical nanofluids, metals like copper, gold, silver, among others. Hayat and Nadeem (2017) investigated heat transfer enhancement with $Ag - CuO$ /water hybrid nanofluid. Swarnalathamma (2018) studied heat and mass transfer on mhd flow of nanofluid with thermal slip effects. Dawar et al. (2018) discussed magnetohydrodynamic CNTs Casson nanofluid and radiative heat transferring a rotating channel. Faraz et al. (2019) studied magnetohydrodynamic impacts on an axisymmetric Casson nanofluid flow and heat transfer over unsteady radially stretching sheet. Anwar et al. (2019) looked into the numerical solution of Casson nanofluid flow over a nonlinear inclined surface with soret and dufour effects by Keller-Box Method. Oke et al. (2020) analyzed the dynamics of non-Newtonian Casson fluid over a rotating non-uniform surface subject to Coriolis force. Gbadeyan et al. (2020) analyzed effect of variable thermal conductivity and viscosity on Casson nanofluid flow with convective heating and velocity slip. Kigio et al. (2021) analysed volume fraction and convective heat transfer on mhd Casson nanofluid over a vertical plate. Anwar et al. (2021) investigated unsteady mhd natural convection flow of Casson fluid incorporating thermal radiative flux and heat injection/suction mechanism under variable wall conditions. ShanthaSheela et al. (2021) reviewed magnetohydrodynamic flow of nanofluids past a vertical plate under the influence of thermal radiation (others include Koriko et al. (2018); Oyem et al., 2021). Convectively heated hydrodynamic stagnation-point flow of a Casson fluid towards a vertically stretching/shrinking sheet was considered by Mutuku and Oyem (2021). They observed that the flow field velocity decreases with increase in magnetic field parameter and Casson fluid parameter. Okello et al. (2021) examined engine oil base (MWCNTs- TiO_2 , MWCNTs- Al_2O_3 , MWCNTs- Cu) hybrid nanofluids for optimal nanolubricant. Qin et al. (2022) investigated the application of nanofluids in rapid methane hydrate formation. Muthukumar et al. (2022) analyzed the impacts of uniform and sinusoidal heating in a nanofluid saturated porous chamber influenced by thermal radiation and magnetic field. Meng et al. (2022) studied fluid flow and heat transfer of carbon nanotubes or grapheme nanoplatelets-based nanofluids in a channel with micro-cylinders. Yun-Xiang et al. (2022) looked into the application of non-uniform heat

source/sink and viscous dissipation in mhd flow of Casson nanoparticles towards a porous stretchable sheet. They observed that velocity of the nanoparticles, decline effectively with porosity parameter and nanoparticles volume fraction. Casson nanofluid flow theoretically over a vertical Riga plate was studied by Khan et al. (2022). They observed that increase in skin-friction caused a rigid compaction of the materials and improves the tensile strength of the concrete.

From the aforementioned literature, more on Casson nanofluid flow past a vertical plate or stretching sheet were discussed with deficit over a vertical plate hence, this study investigates the mhd convective heat transfer of a Casson nanofluid flow over a vertical plate. This is an extension of work of Kigio el al. (2021) to include combined effects of body force, magnetics force and influence of heat source parameter on the Casson nanofluid flow field.

Mathematical Formulation of the Problem

A steady, two-dimensional, incompressible, laminar mhd free convective flow of a Casson nanofluid with heat source over a vertical plate is considered. The Casson nanofluid with base fluid is considered to flow over a vertical plate and subjected to a convective heating boundary condition where, the flow along the along the x-axis is taken in the upward direction and y-axis normal to the plate. The magnetic field B_o is applied normal to the flow direction as shown in Figure 1. The induced magnetic field and viscous dissipation effects are ignored where T_w and C_w are temperature and concentration over the plate; and T_∞ and C_∞ are the free stream temperature and concentration.

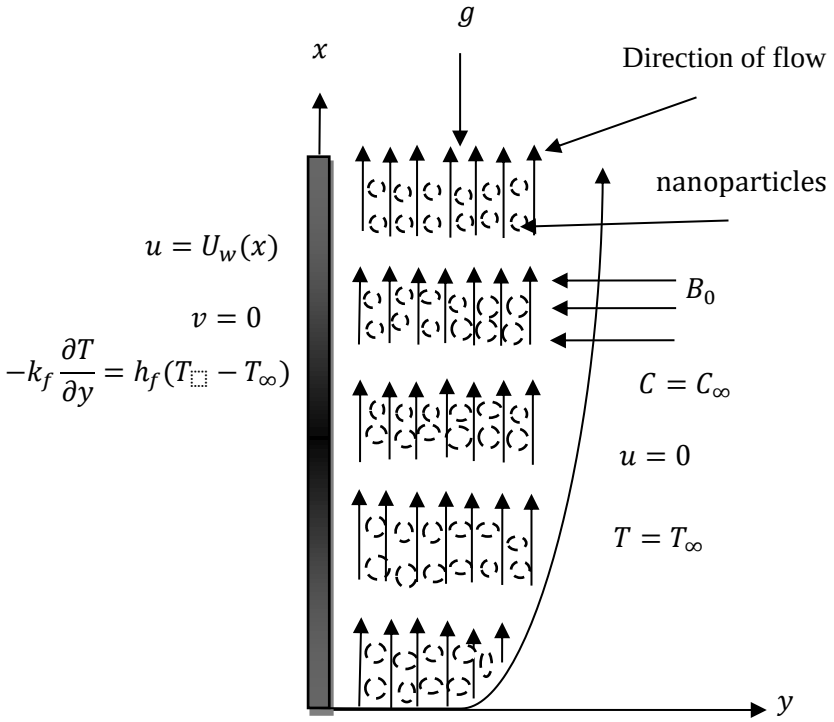

Figure 1: Schematic diagram of the flow

Base on Boussinesq's approximation, the governing partial differential equation of the flow with heat source is given as:

$$\frac{\partial u}{\partial x} + \frac{\partial v}{\partial y} = 0 \quad (1)$$

$$u\frac{du}{dx} + v\frac{du}{dy} = \frac{\mu_{nf}}{\rho_{nf}}\left(1 + \frac{1}{\gamma}\right)\frac{\partial^2 u}{\partial y^2} + g\beta_T(T - T_\infty) + g\beta_C(C - C_\infty) - \frac{\sigma_{nf}B_o^2 u}{\rho_{nf}} \quad (2)$$

$$u\frac{\partial T}{\partial x} + v\frac{\partial T}{\partial y} = \alpha_{nf}\frac{\partial^2 T}{\partial y^2} + \tau\left(D_B\frac{\partial C}{\partial y}\frac{\partial T}{\partial y} + \frac{D_T}{T_\infty}\left(\frac{\partial T}{\partial y}\right)^2\right) + \frac{\mu_{nf}}{(\rho c_p)_{nf}}\left(\frac{\partial u}{\partial y}\right)^2 + \frac{\sigma_{nf}B_o^2 u^2}{(\rho c_p)_{nf}} + \frac{Q_o}{(\rho c_p)_{nf}}(T - T_\infty) \quad (3)$$

$$u\frac{\partial C}{\partial x} + v\frac{\partial C}{\partial y} = D_B\frac{\partial^2 C}{\partial y^2} + \frac{D_T}{T_\infty}\frac{\partial^2 T}{\partial y^2}. \quad (4)$$

The boundary conditions over the vertical plate and free stream are:

$$u = ax,\ v = 0,\ -k_f\frac{\partial T}{\partial y} = h_f(T_f - T),\ C = C_w(x) \quad \text{at} \quad y = 0, \quad (5)$$

$$u \to 0,\ T \to T_\infty,\ C \to C_\infty \quad \text{as} \quad y \to \infty. \quad (6)$$

Where u and v are the velocity components in x, y directions respectively, ρ is the viscosity, nf is the nanofluid parameter, bf is the base fluid of the Casson nanofluid. Applying stream functions $u = \frac{\partial \psi}{\partial x}$ and $v = -\frac{\partial \psi}{\partial y}$ with defined values of $u = axf'(\eta)$ and $v = \sqrt{av}\, f(\eta)$, the continuity equation (1) is satisfied. For ease of computation, thermal conductivity, density, viscosity and specific heat capacity of the nanofluid as defined by Yang et al. (1996), Pak and Cho (1998), Maiga et al. (2004), Kigio et al (2021) were used.

Simplifying further the mathematical problem (2) – (6), the following similarity variables are introduced

$$\eta = y\sqrt{\frac{a}{v}};\ \psi = \sqrt{av}\, xf(\eta);\ T = T_\infty + (T_w - T_\infty)\theta(\eta);\ C = C_\infty + (C_w - C_\infty)\phi(\eta). \quad (7)$$

Using equation (7), equations (2) – (6) are transformed to a set of couple nonlinear ordinary differential equations

$$\frac{\mu_{nf}}{\rho_{nf}\upsilon_{bf}}\left(1+\frac{1}{\gamma}\right)\frac{d^3f}{d\eta^3}-\left(\frac{df}{d\eta}\right)^2+f\frac{d^2f}{d\eta^2}+Gr_t\theta+Gr_s\phi-M\frac{df}{d\eta}=0, \quad (8)$$

$$\frac{d^2\theta}{d\eta^2}+\left(Prf+N_b\frac{d\phi}{d\eta}\right)\frac{d\theta}{d\eta}+N_t\left(\frac{d\theta}{d\eta}\right)^2+PrEc\left(\frac{\mu_{nf}}{\rho_{nf}\upsilon_{bf}}\left(\frac{d^2f}{d\eta^2}\right)^2+M\left(\frac{df}{d\eta}\right)^2\right)+PrQ\theta=0, \quad (9)$$

$$\frac{d^2\phi}{d\eta^2}+Sc\frac{d\phi}{d\eta}f+\frac{N_t}{N_b}\frac{d^2\theta}{d\eta^2}=0. \quad (10)$$

with dimensionless boundary conditions

$$f(0)=0,\ \frac{df}{d\eta}(0)=1,\ \frac{d\theta}{d\eta}(0)=-Bi(1-\theta),\ \phi(0)=0,\ \frac{df}{d\eta}(\infty)\to 0,\ \theta(\infty)\to 0,\ \phi(\infty)\to 0. \quad (11)$$

From the couple nonlinear ordinary differential equations (8) – (10) with boundary conditions (11), prime denotes differentiation with respect to η, and $Gr_t=\frac{g\beta(T_w-T_\infty)}{a^2x}$ is thermal Grashof number, $Gr_s=\frac{g\beta^*(C_w-C_\infty)}{a^2x}$ is the solutal Grashof number, $Sc=\frac{\upsilon}{D_B}$ the Schmidt number, $Ec=\frac{a^2x}{(c_p)_{nf}(T_w-T_\infty)}$ Eckert number, $Pr=\frac{\upsilon_{bf}}{\alpha_{bf}}$ is the Prandtl number, $M=\frac{\sigma_{nf}B_0^2}{\alpha\rho_{nf}}$ the magnetic field, $N_b=\frac{\tau D_B}{\alpha_{nf}}$ Brownian parameter, $N_t=\frac{\tau D_T(T_w-T_\infty)}{\alpha_{nf}T_\infty}$ is the Thermophoretic parameter, $Bi=\frac{h_f}{k_\infty}\sqrt{\frac{a}{\upsilon}}$ is the Biot number, $Q=\frac{q}{p}$ heat source parameter and $Re_x=\frac{v_0x}{\upsilon}$ is the Reynolds number.

The skin-fiction coefficient, Nusselt number and Sherwood number are defined as

$$C_f=\frac{\tau_w}{\rho u_0 v_0}=\frac{\partial u}{\partial y}\Big|_{y=0} \quad (12)$$

$$Nu=x\frac{\frac{\partial T}{\partial y}}{T_w-T_\infty}=\frac{Nu_x}{Re_x}=\frac{\partial\Theta}{\partial y}\Big|_{y=0} \quad (13)$$

$$Sh=\frac{1}{Re_x}=\frac{\upsilon}{v_0x} \quad (14)$$

Numerical Procedure

The couple nonlinear ordinary differential equations (8) – (10) subject to the dimensionless boundary conditions in equation (11) are solved numerically using Runge-Kutta fourth order technique with shooting method and simulated using MatLab software. Equations (8) –(10) are reduced into a system of first order differential equations, that is, set $y_1=f$, $y_2=f'$, $y_3=f''$, $y_4=\theta$, $y_5=\theta'$, $y_6=\phi$, $y_7=\phi'$ such that,

$$\begin{aligned}
y_1' &= y_2\\
y_2' &= y_3\\
y_3' &= -\frac{\rho_{nf}\upsilon_{bf}\gamma}{\mu_{nf}(\gamma+1)}(y_1y_3-y_2^2+Gr_ty_4+Gr_sy_6-My_2)\\
y_4' &= y_5\\
y_5' &= -\left[\Pr\left(y_1y_5+\frac{\mu_{nf}}{\rho_{nf}\upsilon_{bf}}y_3^2+MEcy_2^2+Qy_4\right)+N_by_7y_5+N_ty_5^2\right] \quad (15)\\
y_6' &= y_7\\
y_7' &= -Scy_1y_7-\frac{N_t}{N_b}y_5'
\end{aligned}$$

subject to the initial conditions:

$$y_1(0)=0,\ y_2(0)=1,\ y_3(0)=s_1,\ y_4(0)=s_2,\ y_5(0)=-bi[1-y_4],\ y_6(0)=0,\ y_7(0)=s_3,\ y_2(\infty)=0,\ y_4(\infty)=0,\ y_6(\infty)=0 \quad (16)$$

The numerical computation with a step-size of $\Delta\eta=0.001$ is chosen to satisfy the convergence criterion of 10^{-5} and, the plate surface temperature $\theta(0)$, skin-friction coefficient $f''(0)$, Nusselt number $-\theta'(0)$ and Sherwood number $-\phi'(0)$ were computed and their numerical results are presented in Table 1 with heat source parameter.

Table 1: Computational results of Heat Source, Skin-friction coefficient, Nusselt number and Sherwood number at $Gr_t=1; Gr_s=3; M=3; \emptyset=0.01; Pr=7.62; Ec=0.1; N_t=N_b=0.1; Sc=0.62; Bi=0.1; \gamma=1.$

Q	$Re^{1/2}C_f$	$Re^{-1/2}N_u$	$Re^{-1/2}Sh$
1	-0.4372	-0.0794	1.2861
2.7778	0.0429	-0.323	1.3287
4.5556	0.5019	-0.5593	1.366
6.3333	0.9448	-0.7909	1.399
8.1111	1.3768	-1.2477	1.4563
9.8889	1.8013	-1.4755	1.4818
11.6667	2.2207	-1.704	1.5056
13.4444	2.6368	-1.704	1.5056
15.2222	3.0507	-1.9339	1.5281
17	3.4635	-2.1656	1.5495

RESULTS AND DISCUSSION

The obtained numerical results of some governing thermophysical parameters with values $Gr_t = 1$; $Gr_s = 3$; $M = 3$; $Pr = 7.62$; $Ec = 0.1$; $\phi = 0.01$; $N_t = N_b = 0.1$; $Sc = 0.62$; $Bi = 0.1$; $Q = 0.1$; $n = 2$; $\gamma = 1$ (Kigio et al., 2021) on velocity, temperature and concentration profiles are presented in Figures (2) – (14). From Table 1, it was observed that skin-friction coefficient (C_f) and Sherwood number (Sh) increases with increase in heat source parameter but, decreases in Nusselt number (Nu) with constant values of $Gr_t = 1$; $Gr_s = 3$; $M = 3$; $Pr = 7.62$; $Ec = 0.1$; $N_t = N_b = 0.1$; $Sc = 0.62$; $Bi = 0.1$ and $\gamma = 1$ as shown in Figure 14.

Figures (2) – (4) show the effect of heat source parameter (Q) on velocity, temperature and concentration profiles. It was observed from Figures (2) and (3) that velocity and temperature profiles increases away from the plate towards the free stream boundary layer with increase in heat source parameter but decreases in concentration profiles as heat source increases as shown in Figure (4). Figures (5) – (7), displays the effect of Prandtl number (Pr) on velocity, temperature and concentration profiles. From Figs (5) and (7), the velocity and concentration profiles decrease towards the plate as Pr increases. But for Figure (6), the effect of Prandtl number on temperature profiles, have a dual effect on the temperature profile. Initially, temperature profiles increases away from the plate as Prandtl number increases but later decreases along the plate towards the free stream boundary layer with increasing values of Prandtl number. Prandtl number (Pr) is the ratio of the momentum diffusivity to thermal diffusivity. Hence, a raise in the Prandtl is also a consequence of an increase in momentum diffusivity or reduction in thermal diffusivity.

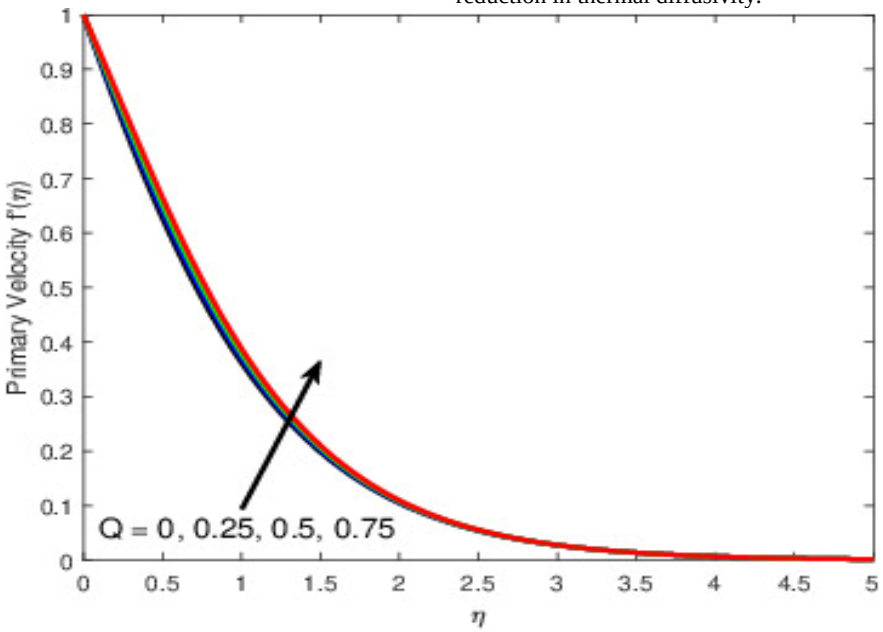

Figure 2: Velocity profiles for Q with $Gr_t = 1$; $Gr_s = 3$; $M = 3$; $Pr = 7.62$; $Ec = 0.1$; $N_t = N_b = 0.1$; $Sc = 0.62$; $Bi = 0.1$; $n = 2$; $\gamma = 1$

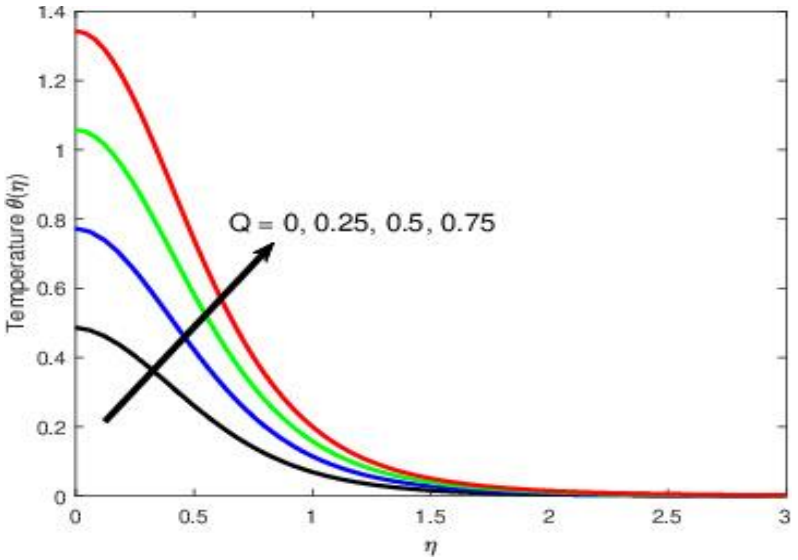

Figure 3: Temperature profiles for Q with $Gr_t = 1$; $Gr_s = 3$; $M = 3$; $Pr = 7.62$; $Ec = 0.1$; $N_t = N_b = 0.1$; $Sc = 0.62$; $Bi = 0.1$; $n = 2$; $\gamma = 1$

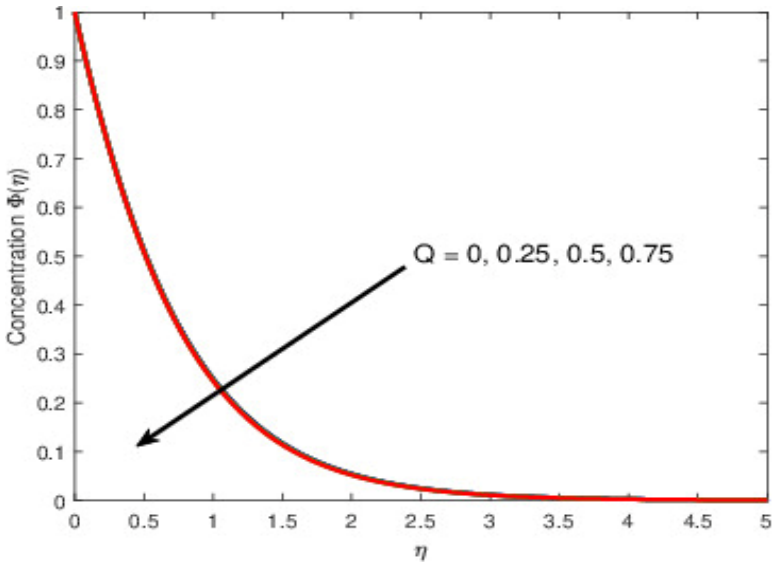

Figure 4: Concentration profiles for Q with $Gr_t = 1$; $Gr_s = 3$; $M = 3$; $Pr = 7.62$; $Ec = 0.1$; $N_t = N_b = 0.1$; $Sc = 0.62$; $Bi = 0.1$; $n = 2$; $\gamma = 1$

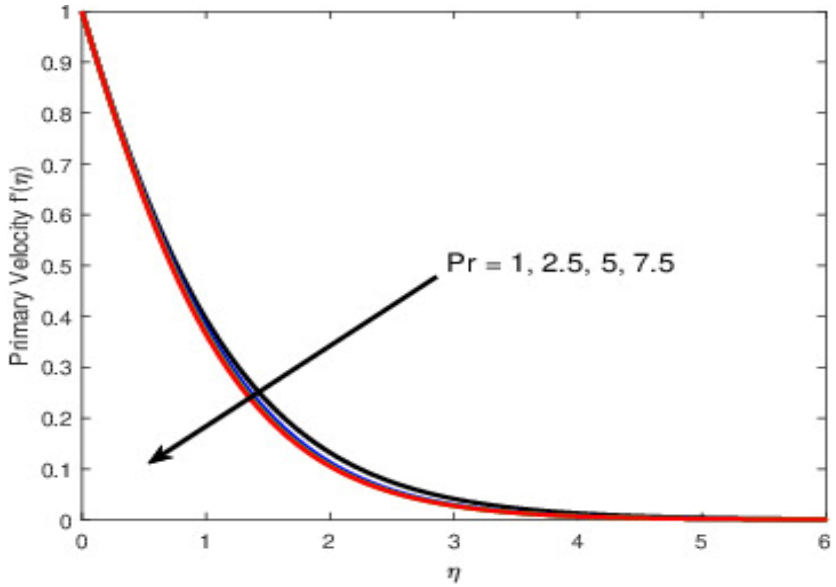

Figure 5: Velocity profiles for Pr with $Gr_t = 1$; $Gr_s = 3$; $M = 3$; $Ec = 0.1$; $N_t = N_b = 0.1$; $Sc = 0.62$; $Bi = 0.1$; $Q = 0.1$; $n = 2$; $\gamma = 1$

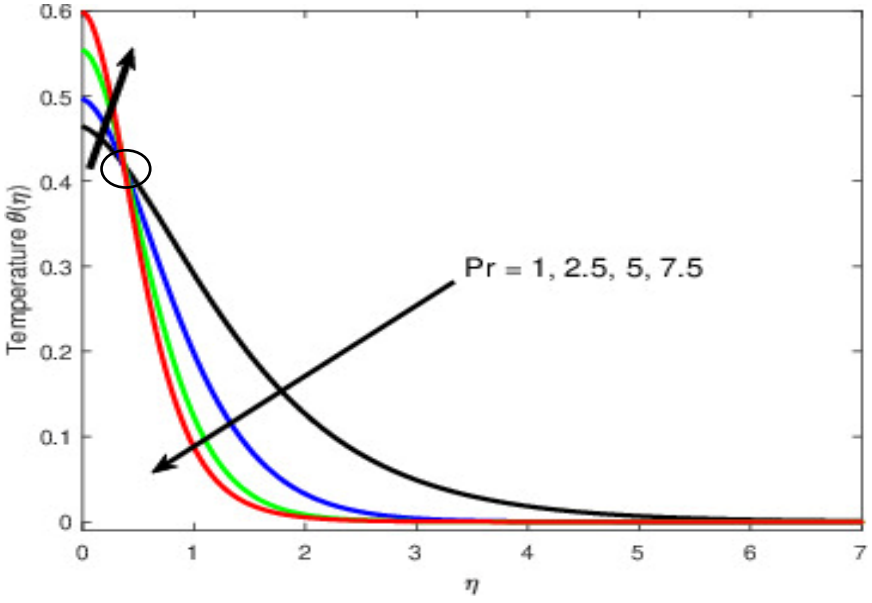

Figure 6: Temperature profiles for Pr with $Gr_t = 1$; $Gr_s = 3$; $M = 3$; $Ec = 0.1$; $N_t = N_b = 0.1$; $Sc = 0.62$; $Bi = 0.1$; $Q = 0.1$; $n = 2$; $\gamma = 1$

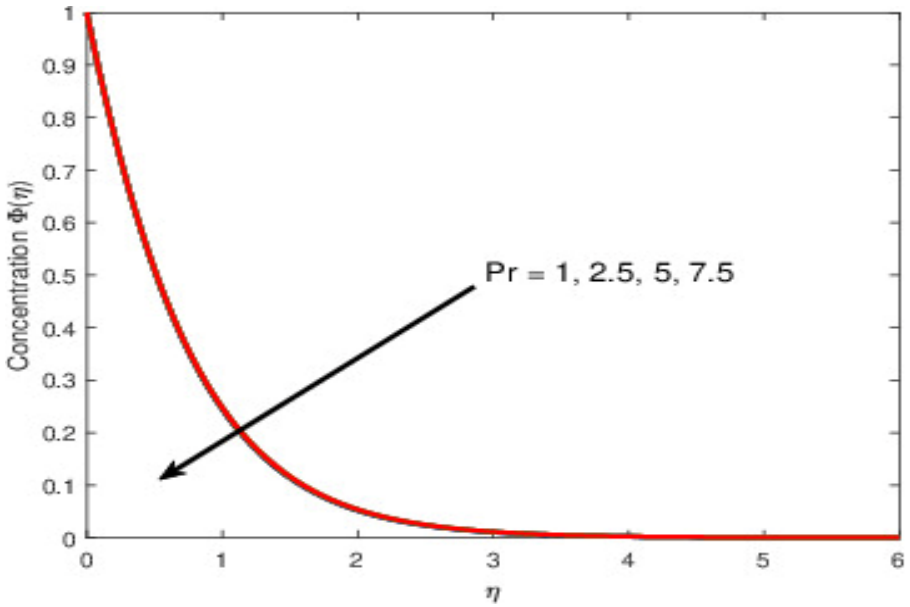

Figure 7: Concentration profiles for Pr with $Gr_t = 1$; $Gr_s = 3$; $M = 3$; $Ec = 0.1$; $N_t = N_b = 0.1$; $Sc = 0.62$; $Bi = 0.1$; $Q = 0.1$; $n = 2$; $\gamma = 1$

The effect of Biot number (Bi), which is measures the internal resistance to heat transfers within a fluid flow, is presented in Figures (8) – (10). It was observed that as Biot number increases, the primary velocity and concentration profiles decreases respectively towards the plate along the thermal boundary layer. Similarly, the flow temperature increases with increasing values of Biot number away from the plate and this result corroborates with the findings of Kigio et al. (2021). Figures (11) – (13) depicts the effect of volume fraction on velocity, temperature and concentration profiles. Increasing the nanoparticle volume fraction, results in the decrease in velocity profiles along the plate (Figure 11) and initially on the temperature profiles but later increases spontaneously away from the plate along the thermal boundary layer in temperature profiles (Figure 12); as it also increases in concentration profiles (Figure 13). This results are in agreement with Kigio et al. (2021) such that, the fluid flow and heat transfer are subdued with increase in nanoparticle volume fraction thereby, causing quick deposition of nanoparticles at the plate.

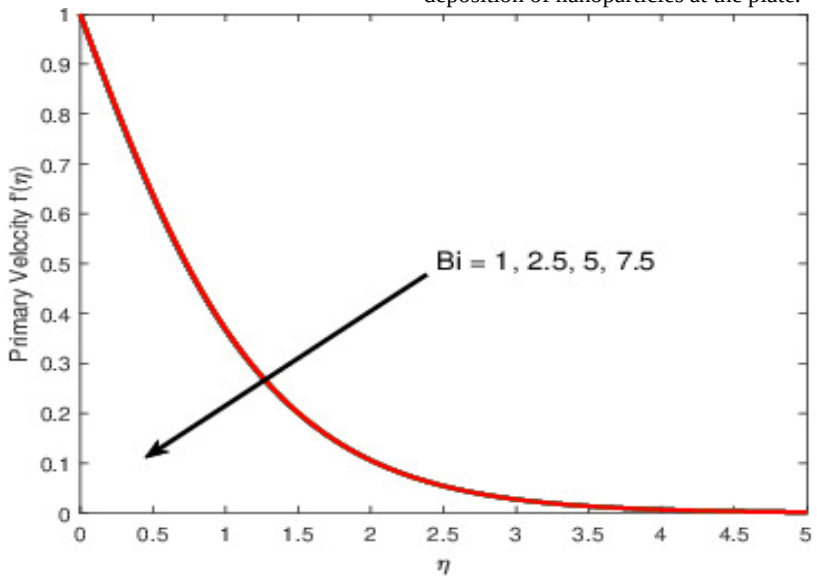

Figure 8: Variation of velocity profiles with Biot number for $Gr_t = 1$; $Gr_s = 3$; $M = 3$; $Pr = 7.62$; $Ec = 0.1$; $\phi = 0.01$; $N_t = N_b = 0.1$; $Sc = 0.62$; $Q = 0.1$; $n = 2$; $\gamma = 1$

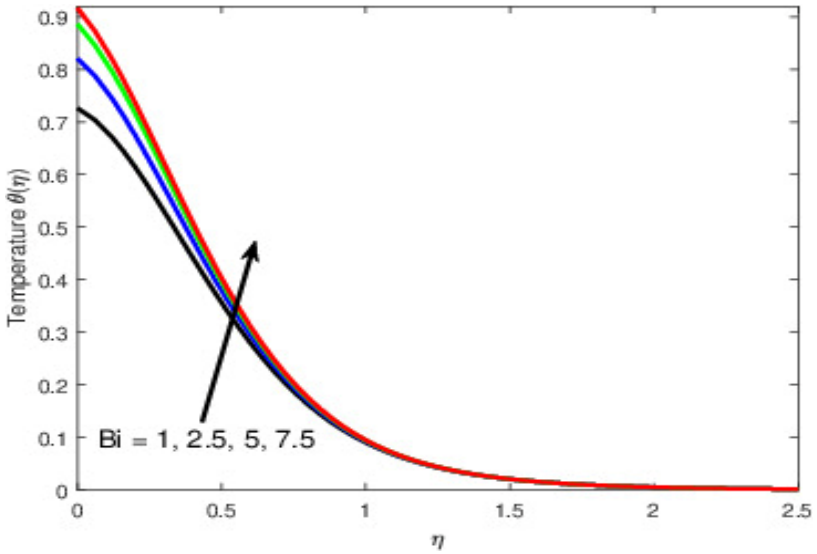

Figure 9: Variation of temperature profiles with Biot number for $Gr_t = 1$; $Gr_s = 3$; $M = 3$; $Pr = 7.62$; $Ec = 0.1$; $\phi = 0.01$; $N_t = N_b = 0.1$; $Sc = 0.62$; $Q = 0.1$; $n = 2$; $\gamma = 1$

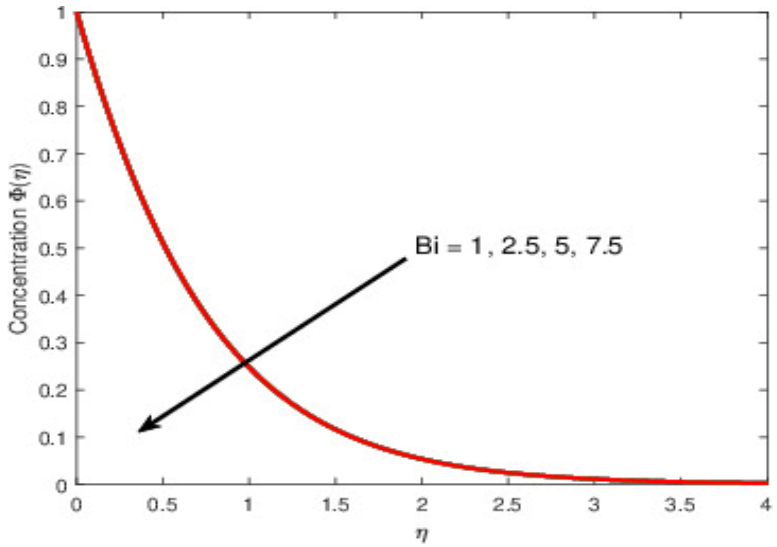

Figure 10: Variation of concentration profiles with Biot number for $Gr_t = 1$; $Gr_s = 3$; $M = 3$; $Pr = 7.62$; $Ec = 0.1$; $\phi = 0.01$; $N_t = N_b = 0.1$; $Sc = 0.62$; $Q = 0.1$; $n = 2$; $\gamma = 1$

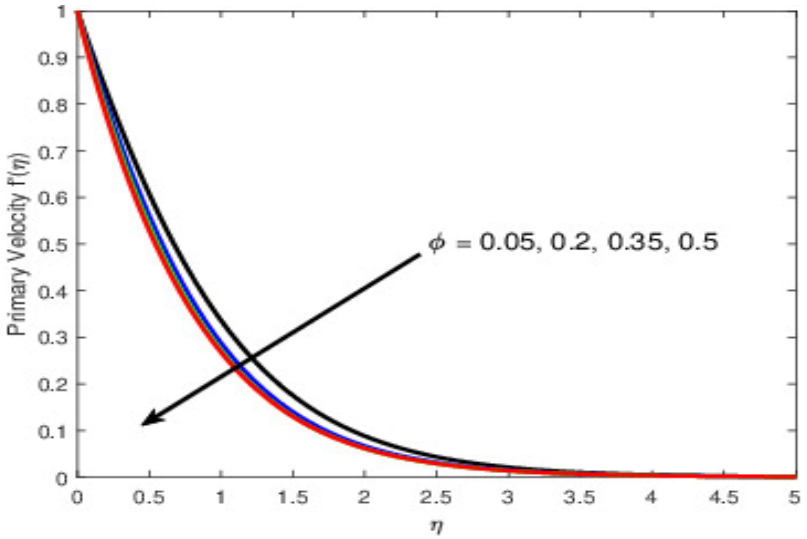

Figure 11: Variation of velocity profiles with volume fraction for $Gr_t = 1$; $Gr_s = 3$; $M = 3$; $Pr = 7.62$; $Ec = 0.1$; $N_t = N_b = 0.1$; $Sc = 0.62$; $Bi = 0.1$; $Q = 0.1$; $n = 2$; $\gamma = 1$

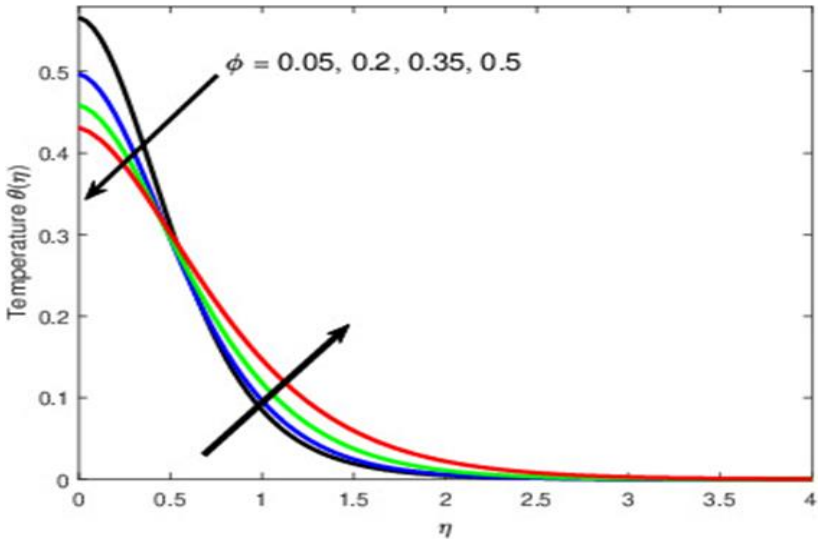

Figure 12: Variation of temperature profiles with volume fraction for $Gr_t = 1$; $Gr_s = 3$; $M = 3$; $Pr = 7.62$; $Ec = 0.1$; $N_t = N_b = 0.1$; $Sc = 0.62$; $Bi = 0.1$; $Q = 0.1$; $n = 2$; $\gamma = 1$

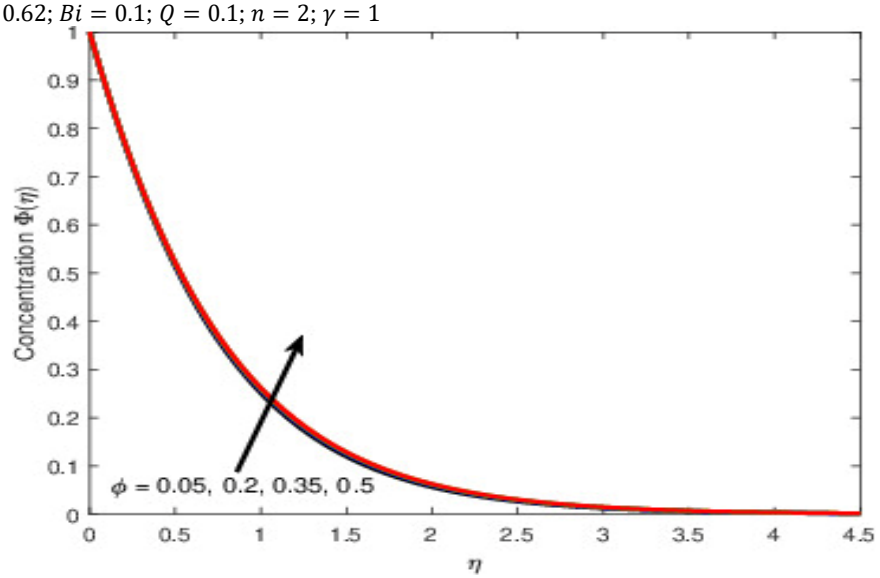

Figure 13: Variation of concentration profiles with volume fraction for $Gr_t = 1$; $Gr_s = 3$; $M = 3$; $Pr = 7.62$; $Ec = 0.1$; $N_t = N_b = 0.1$; $Sc = 0.62$; $Bi = 0.1$; $Q = 0.1$; $n = 2$; $\gamma = 1$

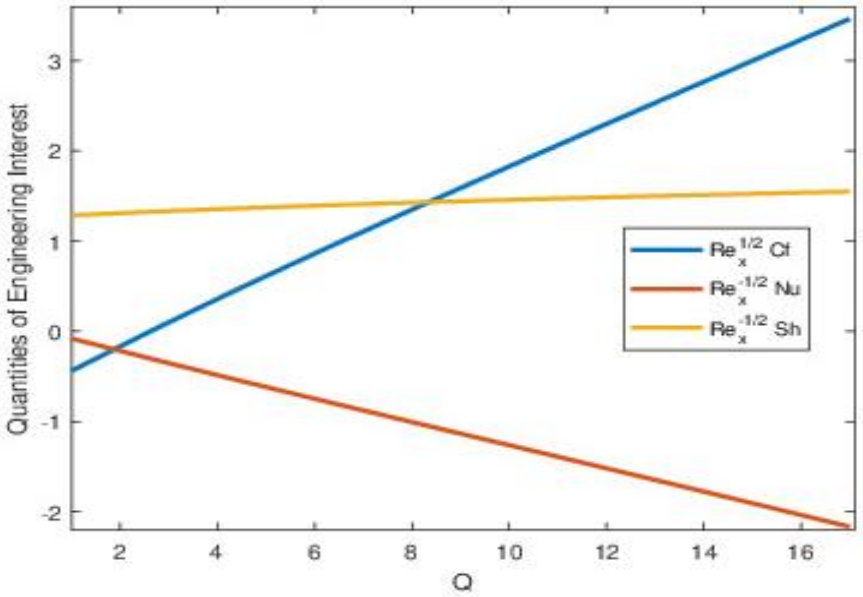

Figure 14: Variation of quantities of interest with heat source parameter at $Gr_t = 1$; $Gr_s = 3$; $M = 3$; $Pr = 7.62$; $Ec = 0.1$; $\phi = 0.01$; $N_t = N_b = 0.1$; $Sc = 0.62$; $Bi = 0.1$; $Q = 0.1$; $n = 2$; $\gamma = 1$

CONCLUSION

A study of Casson nanofluid convective heat flow with heat source parameter over a vertical plate was carried out. The velocity, temperature and concentration profiles for some governing parameters were obtained numerically by Runge-Kutta fourth order technique with shooting method. Their effects on velocity, temperature and concentration profiles were presented graphically and the obtained results revealed that:

i. Heat source parameter increases in terms of skin-friction coefficient and Sherwood number but decreases with Nusselt number.
ii. The velocity boundary layer thickness decreases as Prandtl number, Biot number and volume fraction parameter increases but increases with increasing values of heat source parameter.
iii. The thermal boundary layer thickness increases with heat source parameter, Biot number and volume fraction parameter but decreases with Prandtl number. Similarly, the concentration profiles decreases with Heat source parameter, Prandtl and Biot number respectively but increases with volume fraction parameter.

ACKNOWLEDGEMENT

The authors thank every reviewer for their painstaking effort towards the best output of this article.

CONFLICT OF INTEREST

The authors wish to state that there is no conflict of interest regarding this article and it has not been sent for publication to any journal body.

REFERENCE

Anwar R.K., Misiran M.I., Khan M.I., Alharbi S.O., Thounthong P. and Nisar K. S. (2019): Numerical solution of Casson nanofluid flow over a nonlinear inclined surface with soret and dufour effects by Keller-box method. *Journal of Frontier Physics*, https://dx.doi:10.3389/fphy.2019.00139

Anwar T., Kumam P., and Watthayu W. (2021): Unsteady mhd natural convection flow of Casson fluid incorporating thermal radiative flux and heat injection/suction mechanism under variable wall conditions. *Scientific Reports*, 11(1), 4275. https://doi.org/10.1038/s41598-021-83691-2

Arthur E.M., Seini I.Y. and Bortteir L.B. (2015): Analysis of casson fluid flow over a vertical porous surface with chemical reaction in the presence of magnetic field. *Journal of Applied Mathematics and Physics*, 3(6), https://doi.org/10.4236/jamp.2015.36085

Blair, G. W. S. (1959). An equation for the flow of blood, plasma and serum through glass capillaries. *Nature*, 183**,** 613–614. http://dx.doi.org/10.1038/183613a0

Choi S.U.S. and Eastman J.A. (1995): Enhancing thermal conductivity of fluids with nanoparticles. *ASME International Mechanical Engineering Congress and Exposition, San Francisco*, 12–17

Dawar A., Shah Z., Islam S., Idress M. and Khan W. (2018): Magnetohydrodynamic CNTs Casson nanofluid and radiative heat transfer in a rotating channel. *Int. Journal Phys. Res Appl*., 1, 017-032. https://dx.doi.org/10.29328/journal.jpra.1001002

Faraz F., Haider S. and Imran S.M. (2019): Study of magnetohydrodynamics impacts on an axisymmetric Casson nanofluid flow and heat transfer over unsteady radially stretching sheet. *SN Applied Sciences*, 2(14). https://doi.org/10.1007/s42452-019-1785-5

Gbadeyan J.A., Titiloye E.O., and Adeosun A.T. (2020): Effect of variable thermal conductivity and viscosity on Casson nanofluid flow with convective heating and velocity slip. *Heliyon*, 6(1), e03076.

Hayat T. and Nadeem S. (2017): Heat transfer enhancement with Ag–CuO/water hybrid nanofluid. *Results in Physics*, 7, 2317–2324. https://doi.org/10.1016/j.rinp.2017.06.034

Hussain T., Shehzad S.A., Alsaedi A., Hayat T., Ramzan M., (2015): Flow of Casson nanofluid with viscous dissipation and convective conditions: a mathematical model. *Journal of Central South University*, 22, 1132-1140. https://doi.org/10.1007/s11771-015-2625-4

Khan H., Ali F., Khan N., Khan I. and Mohamed A. (2022): Electromagnetic flow of Casson nanofluid over a vertical Riga plate with ramped wall conditions. *Front. Phys.*, 10. https://doi.org/10.3389/fphy.2022.1005447

Kigio J.K., Mutuku, N.W., and Oke S.A. (2021): Analysis of volume fraction and convective heat transfer on mhd Casson nanofluid over a vertical plate. *Fluid Mechanics***,** 7(1), 1–8. https://doi.org/10.11648/j.fm.20210701.11

Koriko O.K., Oreyeni T., and Oyem O.A. (2018): On the analysis of variable thermophysical properties of thermophoretic viscoelastic fluid flow past a vertical surface with nth order of chemical reaction. *OALib*, 05(6), 1–17. https://doi.org/10.4236/oalib.1104271

Meng G., Chen G., Tan Z., and Wang Z. (2022): Fluid flow and heat transfer of carbon nanotubes- or graphene nano platelets-based nanofluids in a channel with micro-cylinders: an experimental study. *Heat and Mass Transfer*, 58(12), 2221–2234.

Muthukumar S., Sureshkumar S., El-Sapa S., and Chamkha A.J. (2022): Impacts of uniform and sinusoidal heating in a nanofluid saturated porous chamber influenced by the thermal radiation and the magnetic field. *Numerical Heat Transfer, Part A: Applications*, 1–19.

Mutuku W.N. and Oyem A.O. (2021): Casson fluid of a stagnation-point flow (spf) towards a vertical shrinking/stretching sheet. *FUDMA Journal of Sciences*, 5(1), 16-26. https://doi.org/10.33003/fjs-2021-0501-xxx

Oke A.S., Mutuku W.N., Kimathi M., and Animasaun, I.L. (2020): Insight into the dynamics of non-Newtonian Casson fluid over a rotating non-uniform surface subject to Coriolis force. *Nonlinear Engineering*, 9(1), 398–411. https://doi.org/10.1515/nleng-2020-0025

Okello J.A., Oyem A.O., and Mutuku W.N. (2021): Examination of Engin oil-based (MWCNTs- TiO_2 , MWCNTs- Al_2O_3 , MWCNTs- Cu) hybrid nanofluids for optimal nanolubricant. *IOSR Journal of Mathematics*, 17(2), 24-38. https://doi.org/10.9790/5728-1702012438

Oyem O.A., (2015): Effects of thermophysical properties on free convective heat and mass transfer flow over a vertical plate. PhD thesis (unpublished), Department of Mathematical Science, FUTA. Nigeria.

Pramanik S. (2014): Casson fluid flow and heat transfer past an exponentially porous stretching surface in presence of thermal radiation. *Ain Shams Engineering Journal*, 5(1):205–212. https://doi.org/10.1016/j.asej.2013.05.003

Qin Y., Shang L., Zhou L., Zhu J., Yuan S., Zang, C., Ao D., and Li Z. (2022): Application of nanofluids in rapid methane hydrate formation. *A Review Energy Fuels*, 36(16), 8995–9013.

ShanthaSheela J., Gururaj A. D. M., Ismail M. and Dhanasekar, S (2021). Review on magnetohydrodynamic flow of nanofluids past a vertical plate under the influence of thermal radiation. *IOP Conf. Series: Earth and Environmental Science*, 850 012037, https://dx.doi:10.1088/1755-1315/850/1/012037

Sivashanmugam (2012). Application of nanofluids in heat transfer. *Open Science*. http://dx.doi.org/10.5772/52496

Swarnalathamma B.V. (2018): Heat and mass transfer on mhd flow of nanofluid with thermal slip effects. *Int. Journal of Applied Engineering Research*, 13(18), 13705 – 13726

Ullah I., Khan I. and Shafie S. (2016): Mhd natural convection flow of Casson nanofluid over nonlinearly stretching sheet through porous medium with chemical reaction and thermal radiation. *Nanoscale Research Letters*, 11:527. https://dx.doi.10.1186/s11671-016-1745-6

Vijayaragavan R. and Kavitha M.A. (2017): Chemical reacting radiative Casson fluid flow over a vertical plate in the presence of heat source/sink and aligned magnetic field. *Chemical Process Engineering Research*, 49, 14-31

Yun-Xiang Li, Israr Ur Rehman M., Wen-Hua Huang, Ijaz Khan M., Sami Ullah Khan, and Ronnason Chinram, Kadry S., (2022): Dynamics of casson nanoparticles with non-uniform heat source/sink: a numerical analysis. *Ain Shams Engineering Journal*, 13(1), https://doi.org/10.1016/j.asej.2021.05.010

Nomenclature

B_o - Magnetic field strength
C - Concentration of nanoparticle
c_p - Specific heat capacity
C_w - Wall stream concentration
C_∞ - Free stream concentration
g - Accelerated due to gravity
n -Velocity index
T - Temperature of the fluid within the boundary layer
T_w - Wall stream temperature
T_∞ - free stream temperature
u - Velocity component in x– direction
v - Velocity component in y– direction
x - Coordinate along the plate
y - Coordinate normal to the plate

Greek Letters

α - Thermal diffusivity
α_{bf} - Thermal diffusivity of base fluid
α_{nf} - Thermal diffusivity of the nanofluid
β_T- - Coefficient of thermal expansion
β_C - Coefficient of concentration expansion
β - Thermal coefficient of volumetric expansion
β^* - Concentration coefficient
$(\rho c_p)_{np}$ - Heat capacity of the nanofluid
η - Similarity variable
ψ - Stream function
∞ - Evaluation at free stream conditions
ϕ - Dimensionless concentration
σ - Electrical conductivity
υ - Kinematic viscosity
μ- Coefficient of dynamic fluid viscosity
μ_{nf} - Dynamic viscosity of the nanofluid
γ - Casson fluid parameter or Thermal conductivity variation parameter
τ - Shear stress

Subscripts

bf -Base fluid
nf - Nanofluid
np – Nanoparticle